UNIVERSITY OF BIRMINGHAM

Research at Birmingham

Mn-based borohydride synthesized by ball-milling KBH4 and MnCl2 for hydrogen storage

Liu, Ruixia; Book, David

Link to publication on Research at Birmingham portal

Available online at www.sciencedirect.com

ScienceDirect

journal homepage: www.elsevier.com/locate/he

Mn-based borohydride synthesized by ball-milling KBH$_4$ and MnCl$_2$ for hydrogen storage

CrossMark

Ruixia Liu [a,b,*], *David Book* [a]

[a] School of Metallurgy and Materials, University of Birmingham, Edgbaston, Birmingham B15 2TT, UK
[b] State Key Laboratory of Environmental Criteria and Risk Assessment (SKLECRA), Chinese Research Academy of Environmental Sciences, Beijing 100012, China

ARTICLE INFO

ABSTRACT

In this work, a mixed-cation borohydride (K$_2$Mn(BH$_4$)$_4$) with P2$_1$/n structure was successfully synthesized by mechanochemical milling of the 2KBH$_4$−MnCl$_2$ sample under argon. The structural and thermal decomposition properties of the borohydride compounds were investigated using XRD, Raman spectroscopy, FTIR, TGA-MS and DSC. Apart from K$_2$Mn(BH$_4$)$_4$, the KMnCl$_3$ and unreacted KBH$_4$ compounds were present in the milled 2KBH$_4$−MnCl$_2$. The two mass loss regions were observed for the milled sample: one was from 100 to 160 °C with a 1.6 ± 0.1 wt% loss (a release of majority hydrogen and trace diborane), which was associated with the decomposition of K$_2$Mn(BH$_4$)$_4$ to form KBH$_4$, boron, and finely dispersed manganese; the other was from 165 to 260 °C with a 1.9 ± 0.1 wt% loss (only hydrogen release), which was due to the reaction of KBH$_4$ with KMnCl$_3$ to give KCl, boron, finely dispersed manganese. Simultaneously, the formed KCl could dissolve in KBH$_4$ to yield a K(BH$_4$)$_x$Cl$_{1-x}$ solid solution, and also react with KMnCl$_3$ to form a new compound K$_4$MnCl$_6$.

1. Introduction

Borohydrides formed from transition metals with electronegativities between 1.2 and 1.6 are expected to be promising candidates for hydrogen storage [1,2]. Manganese borohydride (Mn(BH$_4$)$_2$) has a theoretical hydrogen content of 9.5 wt% with a thermal decomposition temperature between 130 and 180 °C [2]. Mechanochemical synthesis (ball milling) has successfully been used to synthesize Mn(BH$_4$)$_2$ via a metathesis reaction between lithium borohydride (LiBH$_4$) and manganese chloride (MnCl$_2$) [2–4]. The composition and decomposition properties of resulting materials from ball-milling technique highly depend on the precursors. Although Mn(BH$_4$)$_2$ was also formed through ball milling of NaBH$_4$ with MnCl$_2$ (under optimized conditions), the resulting material (under comparable milling conditions) was poorly crystalline [5] and the formed NaCl, unlike LiBH$_4$ as a precursor, where LiCl as one of resulting products was formed through a complete metathesis reaction [4], subsequently reacted with the remaining NaBH$_4$ and MnCl$_2$ to produce a solid solution of NaCl$_x$(BH$_4$)$_{1-x}$ and an amorphous Na−Mn−(BH$_4$)−Cl phases [5]. These preparations involved a complete or incomplete ion exchange reaction between alkali borohydrides and manganese chloride.

To obtain borohydride complexes with improved thermodynamic properties, one approach is to prepare mixed-cation borohydrides by thermodynamic tuning, which allows the borohydride-based compounds to be synthesized selectively. Combining appropriate cations has been an effective method for adjusting the thermodynamic stability of borohydrides so as to have decomposition temperatures within the desired range for hydrogen storage applications. Several examples, such as $LiK(BH_4)_2$, $ZrLi(BH_4)_5$, $ZrLi_2(BH_4)_6$, $LiSc(BH_4)_4$ and $NaZn_2(BH_4)_5$, have been reported so far [6–9]. For modifying the thermodynamic properties of borohydrides, the mixed-anion borohydrides through the anion substitution between halide anions (F^-, Cl^-, Br^-, I^-) in alkali or alkaline earth salts and BH_4^{-} in metal borohydride structure have been prepared. Dissolution of ACl into ABH_4 (A = Li, Na or K), forming solid solutions such as $Na(BH_4)_{1-x}Cl_x$ [10] and $Li(BH_4)_{1-x}Cl_x$ [11,12], has been observed through ball-milling, annealing or combination of ball-milling and annealing of ABH_4–ACl mixture. The formation of the solid solutions may alter the decomposition pathways, the structural flexibility and reactivity of ABH_4. Therefore, the mixed-ion borohydrides might play an important role in the modification of the thermal decomposition of borohydride compounds.

The bimetallic borohydrides $K_2M(BH_4)_4$ (M = Mg or Mn) and $K_3Mg(BH_4)_5$ have been recently synthesized by Schouwink et al. through mechanochemical ball-milling of the reactants KBH_4 with $M(BH_4)_2$ in different molar ratios, where $Mn(BH_4)_2$ was firstly prepared by the metathesis reaction between $LiBH_4$ and $MnCl_2$ in ether [13]. An in-depth crystallographic and spectroscopic characterization revealed that $K_2M(BH_4)_4$ crystallized as a distorted K_2SO_4-type structure in space group $P2_1/n$. Schouwink et al. also reported that although $K_2Mn(BH_4)_4$ was formed by ball milling of $4KBH_4$–$3MnCl_2$, its structural features were not identical to those of the chlorine-free synthesis, due to the severe peak overlap and the temperature dependent interplay of two polymorphs of the ternary chloride $KMnCl_3$ [13].

The aims of this study are to extend the results from the milled KBH_4–$MnCl_2$ sample to the ternary borohydride (K–Mn–BH_4) system and to provide insight into the decomposition mechanism(s) in detail within the milled multiple polymorphs so as to facilitate the development of reversible hydrogen sorption reaction pathways. The milled $2KBH_4$–$MnCl_2$ sample is investigated by X-ray diffraction (XRD), vibrational spectroscopy (Raman and FTIR), thermal analysis (TGA-MS and DSC).

2. Experimental method

2.1. Materials and synthetic method

Potassium borohydride (KBH_4, >98%) and anhydrous manganese chloride ($MnCl_2$, 99.999%) were obtained from Sigma–Aldrich Company ltd. All the materials and prepared samples were stored and handled in an argon (99.99% purity) filled glovebox (MBraun Labstar). The levels of water and oxygen in the glovebox were kept below 0.1 ppm and the hydrogen level was less than 0.1%.

A 6 g mixture of KBH_4 and $MnCl_2$ in 2:1 molar ratios was put in a stainless steel milling bowl (250 ml) and sealed under argon with a lid using a Viton O-ring. The mass ratio of the stainless steel balls (14 mm diameter) to powder was approximately 32:1. At room temperature, the mixture was milled using a Retsch PM400 Planetary Ball Mill at 175 rpm. In order to reduce the amount of heat generated, milling was carried out in 36 × 10 min durations separated by 10 min rest intervals, giving total milling times of 360 min.

2.2. XRD characterization

The crystal properties of milled samples were investigated using a Bruker D8 Advance X-ray Diffractometer with Cu Kα radiation (λ = 0.154 nm). An Anton Parr XRK900 high-temperature sample cell was used to measure the temperature dependent properties of samples heated at 2 °C/min under 3 bar He flowing at 100 ml/min.

TOPAS software supplied by Bruker AXS [14], jEdit obtained from Durham University website managed by Prof. John Evans [15] and Crystallographic Information Files (.cif) from the Chemical Crystal Database [16], were used for the analysis of the polymorphs present in the XRD pattern of prepared samples.

2.3. Raman and IR analysis

Raman spectra were obtained using a Renishaw inVia Raman Microscope with Ar ion laser power (2 mW, 488 nm). A microscope objective was used to focus the laser beam onto the sample with a spot-diameter of about 50 μm. The Raman scattered light ranged between 100 and 4000 cm^{-1} was collected using a 2400 grooves/mm grating. The spectral resolution was 2–4 cm^{-1}. The number of scans was optimized for each sample to obtain high intensity and well-resolved Raman spectra. In an Ar glovebox, the sample was loaded into an Instec HCS621V sample cell stage, preventing contact between the sample and the air. The temperature-dependent Raman spectra were measured by heating sample at 2 °C/min in 1 bar Ar flowing at 100 ml/min.

IR spectroscopic measurements were performed with a Nicolet 8700 Fourier Transform Infrared (FTIR) spectrometer using an attenuated total reflectance (ATR) attachment that allowed inert loading of samples. The spectrometer was purged with high-purity nitrogen for 30 min prior to measurements in order to try to minimize the carbon dioxide and water level within the spectrometer. The spectral resolution was 4 cm^{-1}, and a spectral range of 500–4000 cm^{-1} was selected. For FTIR measurements, the powder samples were pressed onto the crystal (of the 'Golden Gate') with a calibrated torque and sealed in the sample holding cell in the glovebox.

2.4. Thermal analysis

The thermal decomposition behaviour of the milled mixtures was investigated by thermogravimetric analysis (TGA, Netzsch TG209) with the exhaust gas analysed by mass spectrometry (MS, Hiden Analytical HAL IV). Approximately 10–15 mg of sample was placed in an aluminium oxide crucible and covered with a lid. The sample was heated from 30 to

500 °C with heating rate of 2 °C/min under 1.5 bar argon flowing at 40 ml/min. Before a sample measurement, a baseline was run using an empty crucible under the same conditions as a sample measurement, so as to subtract any buoyancy effects on heating.

The MS was set up to measure the concentrations of H_2 ($m/z = 2$) and B_2H_6 ($m/z = 26$). However, it should be noted that a proportion of any B_2H_6 evolved may have been deposited onto the surfaces of the connecting pipe between the TGA and MS, lowering the concentration values for B_2H_6.

Differential scanning calorimetry (DSC, Netzsch DSC204HP) was performed on a pre-weighed sample of approximately 10 mg in an Al crucible heated from 30 to 500 °C. A temperature ramp rate of 2 °C/min and 4 bar argon flowing at 100 ml/min were used for all the measurements. Before the sample measurement, a baseline was conducted using an empty Al pan under the same conditions as the sample measurement to reduce the effect of background on the sample measurement.

3. Results and discussion

3.1. XRD of the milled material

Powder XRD was performed on the milled $2KBH_4$–$MnCl_2$ sample, as shown in Fig. 1. There are three major polymorphs, identified as orthorhombic $KMnCl_3$(o) ($a = 8.79$ (4) Å, $b = 3.88$ (5) Å, $c = 14.42$ (2) Å) [17], cubic KBH_4 ($a = 6.715$ (6) Å) and $K_2Mn(BH_4)_4$ with a space group of $P2_1/n$ ($a = 8.1347$ (5) Å, $b = 9.860$ (6) Å, $c = 12.768$ (8) Å, $\beta = 100.530(6)°$) [13]. The structure of the $K_2Mn(BH_4)_4$ compound was reported by Schouwink et al. [13], who used synchrotron radiation powder X-ray diffraction (SR-PXD) to identify the structure of $K_2Mn(BH_4)_4$ compound. A mixed-cation borohydride $KSc(BH_4)_4$ and mixed-anion and -cation borohydride compound $KZn(BH_4)Cl_2$ have also been prepared through ball milling of both KBH_4 with $ScCl_3$ and KBH_4 with $ZnCl_2$ respectively [18,19]. Accordingly, the synthetic process of ball milling of the KBH_4–$MnCl_2$ sample with 2:1 molar ratio can be proposed via Equation (1), giving excess KBH_4 in the milled sample:

$$4KBH_4 + 3MnCl_2 \rightarrow 2KMnCl_3(o) + K_2Mn(BH_4)_4 \qquad (1)$$
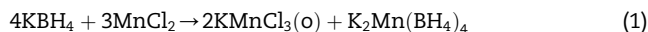
3.2. Spectroscopic properties of the milled sample

Raman spectra of milled samples of $2KBH_4$–$MnCl_2$ and KBH_4 are shown in Fig. 2. In the B–H stretching region, the spectrum of KBH_4 consists of strong band at 2305 cm^{-1}, overtones located at 2183, 2210 and 2495 cm^{-1}, and a combination band at 2380 cm^{-1} [20]. After ball milling of KBH_4 with $MnCl_2$, the intensity of the strongest band at 2305 cm^{-1} for KBH_4 decreases dramatically with no significant change in Raman frequency. The superposition of two overtones at 2175 and 2206 cm^{-1}, as well as doublet bands at 2380 and 2408 cm^{-1} are observed in the milled $2KBH_4$–$MnCl_2$ sample. An overtone for KBH_4 at 2495 cm^{-1} is not present in the milled $2KBH_4$–$MnCl_2$ sample. In addition to the bending modes at 1248 and 1118 cm^{-1} in both milled KBH_4 and $2KBH_4$–$MnCl_2$ samples, the two new vibration modes at 1342 and 1035 cm^{-1} are observed only for the milled $2KBH_4$–$MnCl_2$ sample. These results indicate that the Raman spectrum of the milled $2KBH_4$–$MnCl_2$ sample is associated with two separate borohydride environments: one from excess KBH_4 and the other from the newly formed $K_2Mn(BH_4)_4$ with three additional Raman frequencies at 1035, 1342 and 2408 cm^{-1}. This is in agreement with the results reported by Schouwink et al. [13].

Upon cooling the milled $2KBH_4$–$MnCl_2$ sample to −190 °C, a significant modification of the Raman vibration modes is observed, i.e. showing an increase in the intensities of the vibration peaks and a decrease in the peak widths. In addition, the splitting of B–H stretching vibration bands at −190 °C for the milled $2KBH_4$–$MnCl_2$ sample produces three more vibration modes (at 2235, 2288 and 2500 cm^{-1}) than those at room temperature. The Raman frequency shift and the peak splitting at low temperature are due to the reduction of the thermal expansion and fluctuation within a lattice. The thermal vibration causes uniform displacement of molecules and coupling between vibrations within the molecules [21,22].

Fig. 3 shows FTIR spectra of the milled $2KBH_4$–$MnCl_2$ and KBH_4 samples. There are nine vibration bands displayed in the IR spectrum of milled $2KBH_4$–$MnCl_2$ sample, four of which, at
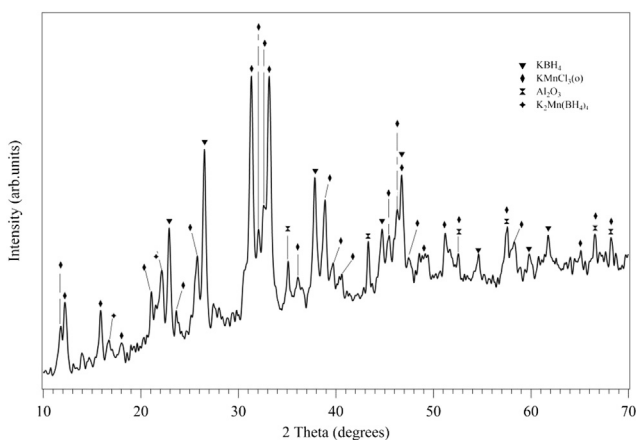

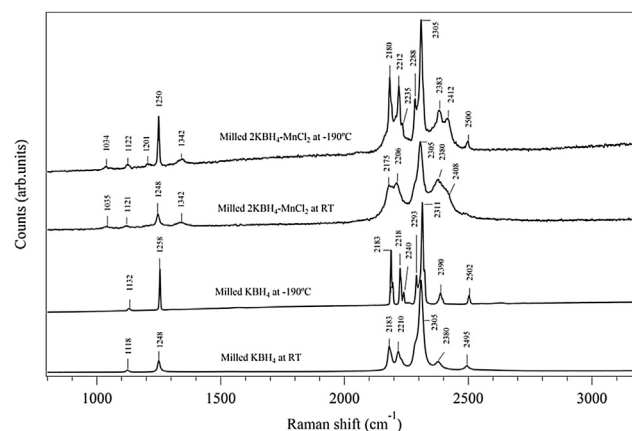Fig. 1 – XRD pattern (Anton Parr cell) of the milled $2KBH_4$–$MnCl_2$ sample.

Fig. 2 – Raman spectra of the milled $2KBH_4$–$MnCl_2$, measured at RT and −190 °C (with 360-min milled KBH_4 at −190 °C, as a reference).

1118, 2210, 2282 and 2273 cm^{-1}, are related to excess KBH_4 in spite of a slight shifting in peak position compared to the pure KBH_4. The other five vibration modes, located at 1038, 1204, 1342, 2174 and 2428 cm^{-1}, are associated with $K_2Mn(BH_4)_4$.

The combination of vibration spectroscopy and XRD results confirms that the $K_2Mn(BH_4)_4$ borohydride complex is formed through ball milling of $2KBH_4$–$MnCl_2$ with excess KBH_4 according to Equation (1).

3.3.   Thermal decomposition

Fig. 4 shows TGA profiles of the milled $2KBH_4$–$MnCl_2$ samples coupled with mass spectra. The two main mass loss regions are observed for the milled samples: one is from 100 to 160 °C with a mass loss of 1.6 ± 0.1 wt%, which is associated with the decomposition of the formed $K_2Mn(BH_4)_4$ compound; the other is from 165 to 260 °C with a mass loss of 1.9 ± 0.1 wt%, which is possibly due to the decomposition of KBH_4 within the mixture. The mass losses in the two regions are accompanied by the release of hydrogen. A trace amount of diborane is detected by MS during the first decomposition process of the milled $2KBH_4$–$MnCl_2$ sample. The first hydrogen evolution is observed at 135 °C for the milled $2KBH_4$–$MnCl_2$. The second hydrogen release around 165–260 °C seems to have large doublets at 210 and 230 °C for the milled sample, suggesting that a multi-step decomposition process occurs.

DSC profiles of the milled $2KBH_4$–$MnCl_2$ samples show that on heating from room temperature to 500 °C, there are several major endothermic and exothermic reactions as shown in Fig. 5: exothermic peaks at 115 °C and endothermic peaks at 129, 203, 214, 231, and 451 °C. DSC results in conjunction with mass spectrometry suggest that the endothermic DSC peak at 129 °C is due to the decomposition of the $K_2Mn(BH_4)_4$ compound, accompanied by hydrogen evolution with a trace amount of diborane. The peaks at 203, 214 and 231 °C are associated with the second multi-step decomposition reaction within the mixture by desorbing hydrogen, which is consistent with TGA results. The exothermic peaks before the decomposition at 115 °C are not accompanied by the release of hydrogen, possibly due to the dissociation of $K_2Mn(BH_4)_4$ to form new polymorphs. The sharp endothermic peak at 451 °C

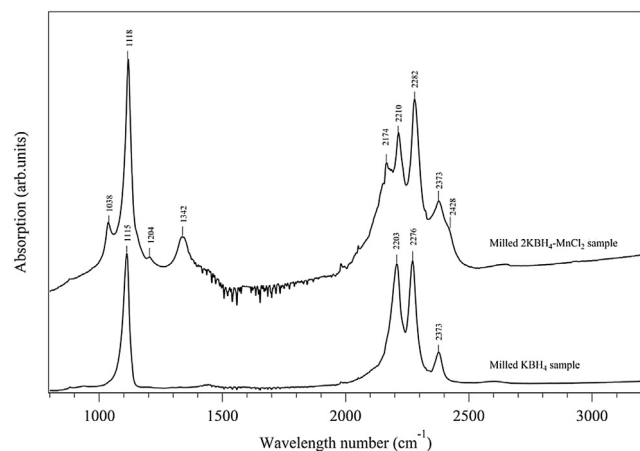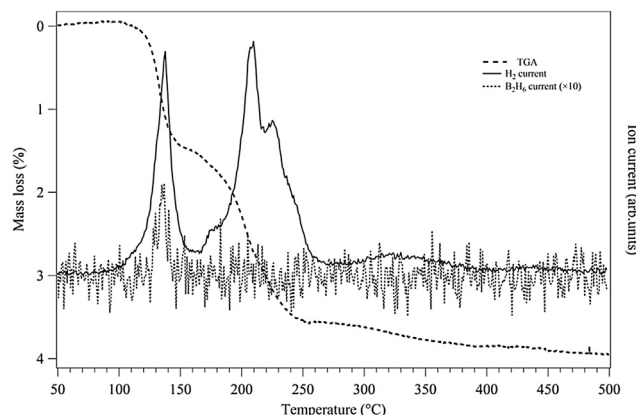**Fig. 4** – TGA coupled with mass spectrometry of the milled $2KBH_4$–$MnCl_2$ sample.

can be related to a phase change in one of the final decomposition products.

3.4.   Decomposition behaviour

Fig. 6 shows *in-situ* XRD patterns of the milled $2KBH_4$–$MnCl_2$ sample in the temperature range of 30–500 °C. At room temperature, the XRD pattern indicates the presence of $KMnCl_3$, $K_2Mn(BH_4)_4$ and KBH_4. Upon heating, the very weak diffraction peaks corresponding to $K_2Mn(BH_4)_4$ at 16.7 and 22.1° 2θ disappear above 120 °C, due to decomposition of the $K_2Mn(BH_4)_4$ complex. This corresponds to the endothermic DSC peaks at around 129 °C and TGA mass losses between 100 and 158 °C with hydrogen and diborane evolution. Simultaneously, an increase in the intensity of the diffraction peaks for KBH_4 occurs between 100 and 160 °C, suggesting that the $K_2Mn(BH_4)_4$ compound decomposes to form KBH_4. Schouwink et al. also found that the decomposition of the $K_2Mn(BH_4)_4$ compound resulted in the formation of KBH_4 and a further new polymorph with weak XRD reflections which has been identified as $KMn(BH_4)_3$ (however, the XRD data was not clear enough to allow the accurate crystal structure to be solved) [13]. Although the KBH_4 compound is formed during the
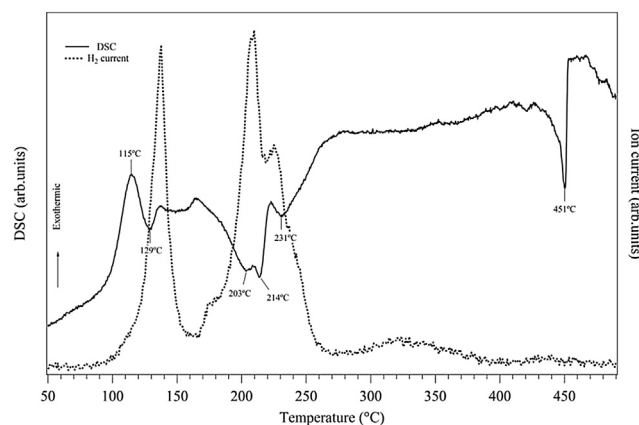

Fig. 3 – FTIR spectra of the milled $2KBH_4$–$MnCl_2$ and KBH_4 samples.

Fig. 5 – DSC and mass spectrometry of the milled $2KBH_4$–$MnCl_2$ sample.
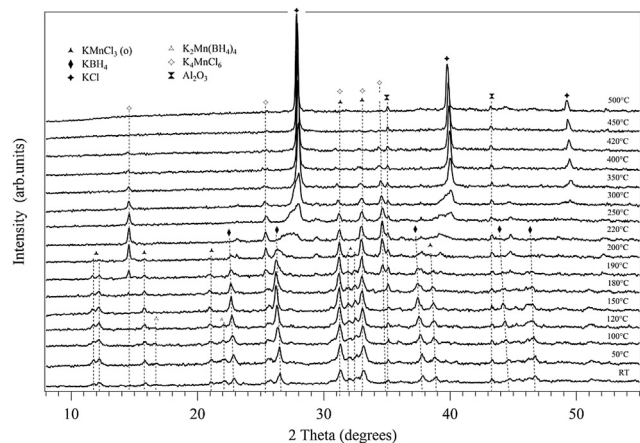
Fig. 6 — *In-situ* XRD of the milled 2KBH$_4$–MnCl$_2$ sample.

decomposition of K$_2$Mn(BH$_4$)$_4$ in this study, peaks for KMn(BH$_4$)$_3$ are not observed in the *in-situ* XRD pattern (Fig. 6). However, an exothermic peak at 115 °C in the DSC profile may be related to the decomposition of K$_2$Mn(BH$_4$)$_4$ to form KBH$_4$ and KMn(BH$_4$)$_3$.

On the other hand, the lattice parameter (*a*) of KBH$_4$ linearly increases from room temperature to 150 °C (due to thermal expansion) then tends to constant between 150 and 170 °C, thereafter the lattice parameter (*a*) of KBH$_4$ reduces (Fig. 7). This result indicates that a proportion of the BH$_4^-$ ions within KBH$_4$ are substituted by Cl$^-$ ions from 150 °C to form a BH$_4^-$ -rich K(BH$_4$)$_{1-x}$Cl$_x$ solid solution. The formation of the KBH$_4$ compound has also been observed during the decomposition of KSc(BH$_4$)$_4$ prepared by Černý et al. [18]. They reported that no Cl$^-$ ions substitution in KBH$_4$ was observed from room temperature to 220 °C, however, a significant substitution occurred at 220–320 °C.

On further heating, the diffraction peaks of KBH$_4$ gradually broaden in width, decrease in intensity and shift in peak position. Simultaneously, the reflections of KMnCl$_3$ reduce and new diffraction peaks at 14.6, 25.3, 31.2, 33.0 and 34.8° 2θ are observed, possibly due to K$_4$MnCl$_6$. With continued heating, the X-ray reflections of K(BH$_4$)$_{1-x}$Cl$_x$ slowly approach the

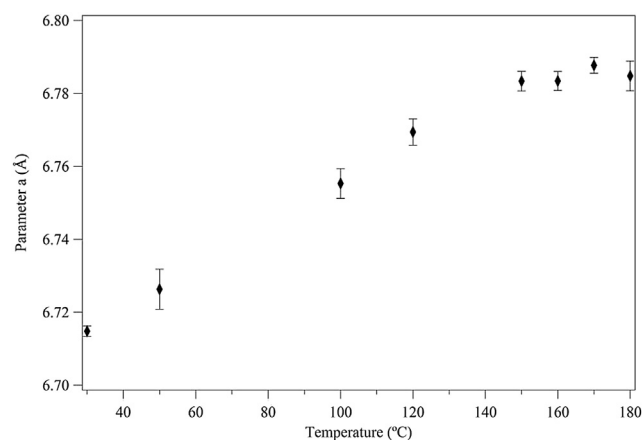diffraction positions of KCl-type, suggesting more Cl$^-$ substituting for BH$_4^-$. All the diffraction peaks disappear completely other than those of KCl above 450 °C. These results suggest that between 165 and 260 °C, three processes occur: the ternary chloride KMnCl$_3$ reacts with KBH$_4$ to produce KCl and possible finely dispersed manganese, boron or borane species (accompanied by hydrogen evolution in multiple steps); some of the produced KCl dissolve in KBH$_4$ to form a K(BH$_4$)$_x$Cl$_{1-x}$; and some of the produced KCl react with KMnCl$_3$ to form K$_4$MnCl$_6$. These results are reasonably in agreement with the two mass loss steps in the TGA profile and several DSC peaks between 170 and 250 °C.

In addition to the reflections of KCl above 450 °C, the diffraction peaks due to the K$_4$MnCl$_6$ compound are absent, most likely due to the decomposition and melting of K$_4$MnCl$_6$ at this temperature [23], which corresponds to a significant endothermic DSC peak at 451 °C.

The thermal decomposition of K$_2$Mn(BH$_4$)$_4$ in this study is very similar to that of KSc(BH$_4$)$_4$ prepared by ball milling of KBH$_4$ and ScCl$_3$ [18]. In both cases, KBH$_4$ is formed during the first decomposition of the complex borohydrides with the concurrent release of hydrogen. The KBH$_4$ then reacts with K–Mn(Sc)–Cl, resulting in a second hydrogen evolution and the formation of KCl. The formed KCl compound then subsequently dissolves in the remaining KBH$_4$ to give a K(BH$_4$)$_{1-x}$Cl$_x$ solid solution.

Fig. 8 shows *In-situ* Raman spectra of the milled 2KBH$_4$–MnCl$_2$ sample during heating. A decrease in intensity for each B–H vibration mode is observed with increasing temperature. On heating sample to 120 °C, the external vibrations, the stretching mode at 2408 cm^{-1} and the bending bands at 1342 and 1035 cm^{-1} disappear, which corresponds to the decomposition of the formed mixed-ions compound K$_2$Mn(BH$_4$)$_4$. At 120 °C, there are still B–H stretching bands at 2175, 2205, 2306 and 2380 cm^{-1}, as well as a bending band at 1248 cm^{-1}, which are all associated with the unreacted KBH$_4$ compound. These vibration modes exist until 220 °C, when KBH$_4$ reacts with ternary chlorides (i.e. KMnCl$_3$) to release hydrogen, consequently leading to the disappearance of the B–H bands in the borohydride compound. These observations agree with the *in-situ* XRD results (Fig. 6).
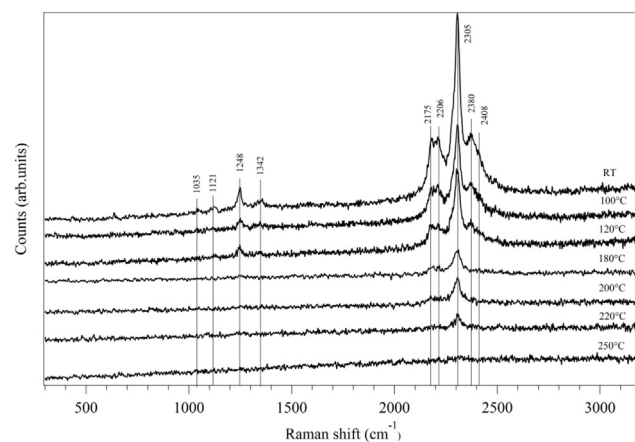

Fig. 7 — The lattice parameter (a) for KBH$_4$ versus temperature (error bars show 3ESDs).

Fig. 8 — *In-situ* Raman spectra of the milled 2KBH$_4$–MnCl$_2$ sample.

Fig. 9 shows the FTIR spectra of the milled $2KBH_4$–$MnCl_2$ sample heated to 150, 250 and 450 °C then cooled to room temperature. The milled sample heated to 150 °C indicates that five modes at 1038, 1204, 1342, 2174 and 2428 cm^{-1} disappear due to the decomposition of $K_2Mn(BH_4)_4$; and four B—H bands at 1118, 2210, 2282 and 2373 cm^{-1} corresponding to KBH_4, and vibration modes at 1246 and 1365 cm^{-1} due to B—B bonding are observed. On further heating to 250 °C, a significant shifting of the four B—H bands from KBH_4 are observed, which corresponds to the dissolution of KBH_4 in KCl to form a $K(BH_4)_{1-x}Cl_x$ solid solution. This observation is consistent with the in-situ XRD patterns, where the reflections for KBH_4 slowly approach those of KCl. Apart from the B—H bands due to $K(BH_4)_{1-x}Cl_x$ solid solution and the B—B bands at 928, 1263 and 1346 cm^{-1} for the decomposed sample at 250 °C, there is a very weak vibration mode at 2478 cm^{-1}, which is possibly due to the reaction of $K(BH_4)_{1-x}Cl_x$ with ternary chloride to form a borane species ($K_2B_{12}H_{12}$), however, the peaks at 1070 and 720 cm^{-1}, which would be expected for $K_2B_{12}H_{12}$ [24], are not observed.

A borane compound is not observed in the in-situ XRD pattern (perhaps owing to a small relative proportion and/or lack of crystallinity), however, it is suggested that, due to the DSC profiles with several endothermic peaks between 170 and 260 °C and the mass spectra of the milled sample with a multi-step hydrogen release, the intermediate compounds may be formed during the thermal decomposition process. The decomposed sample at 450 °C shows that there are no B—H bands owing to KBH_4, or $K(BH_4)_{1-x}Cl_x$, however, very weak vibration modes at 1075 and 2470 cm^{-1} corresponding to borane species and broad bands at 925, 1239 and 1351 cm^{-1} associated with B—B bonding are present.

Although there are no Raman vibration modes observed for the milled $2KBH_4$–$MnCl_2$ samples decomposed respectively at 150, 250 and 450 °C, after being exposed to air at room temperature, these samples exhibit a shark peak at 641 cm^{-1} (Fig. 10), which is believed to be due to the vibrational mode for a manganese oxide [25]. This result indirectly implies that finely dispersed manganese is formed during the decomposition of milled $2KBH_4$–$MnCl_2$ sample.

Fig. 10 – Raman spectra of the milled $2KBH_4$–$MnCl_2$ sample heated to 150, 250 and 450 °C under Ar flowing then exposed to air at RT for 2 min.

Therefore, through the combination of thermal analysis, in-situ XRD measurement, Raman and IR spectrometry, the first thermal decomposition of the milled $2KBH_4$–$MnCl_2$ sample between 100 and 160 °C can be described in Equation (2):

$$K_2Mn(BH_4)_4 \rightarrow 2KBH_4 + Mn + 12/7B + 1/7B_2H_6 + 25/7H_2 \quad (2)$$
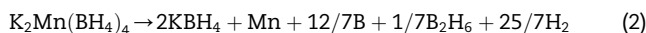
where the theoretical mass loss (1.58 wt%) in the mixture is consistent with the experimental data (1.6 wt%).

In the second thermal decomposition between 165 and 260 °C, there are several reactions taking place simultaneously: the reaction of KBH_4 with ternary chloride to release hydrogen and to form KCl, boron, finely dispersed manganese and possibly small amounts of higher borane species (Equation (3)) with the theoretical mass loss of 1.96 wt% in the mixture, which is consistent with the experimental data (1.9 wt%); the dissolution of KBH_4 in KCl to form the solid solution as expressed in Equation (4); and the transformation of ternary chloride as shown in Equation (5).

$$2KMnCl_3 + 4KBH_4 \rightarrow 6KCl + 2Mn + (4 - 2y/z)B + 7H_2$$
$$+ 2/z[B_yH_z] \quad (3)$$

$$xKCl + (1 - x)KBH_4 \rightarrow K(BH_4)_{1-x}Cl_x \quad (4)$$

$$KMnCl_3 + 3KCl \rightarrow K_4MnCl_6 \quad (5)$$

4. Conclusions

For the milled $2KBH_4$–$MnCl_2$ sample, unlike ABH_4(A = Li and Na) as precursors, there are no distinct X-ray reflections associated with the $Mn(BH_4)_2$ compound. Characterization of the milled materials shows mixed-ion borohydride $K_2Mn(BH_4)_4$, ternary chloride $KMnCl_3$ and unreacted KBH_4 polymorphs. The $K_2Mn(BH_4)_4$ compound has XRD reflections consistent with the $P2_1/n$ structure proposed by Schouwink et al. [13].

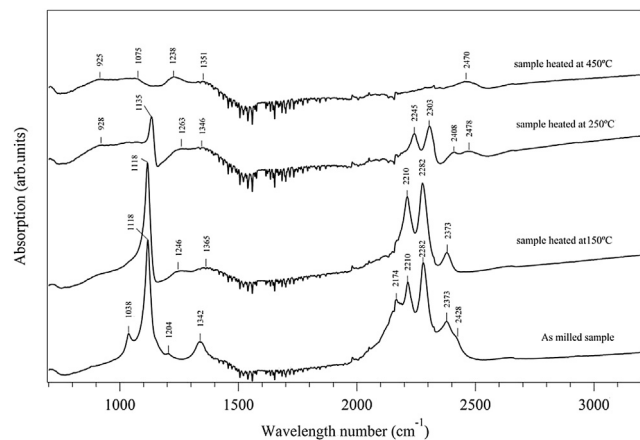**Fig. 9 – FTIR spectra of the milled $2KBH_4$–$MnCl_2$ after heating to 150, 250 and 450 °C under Ar flowing (as-milled sample as a reference).**

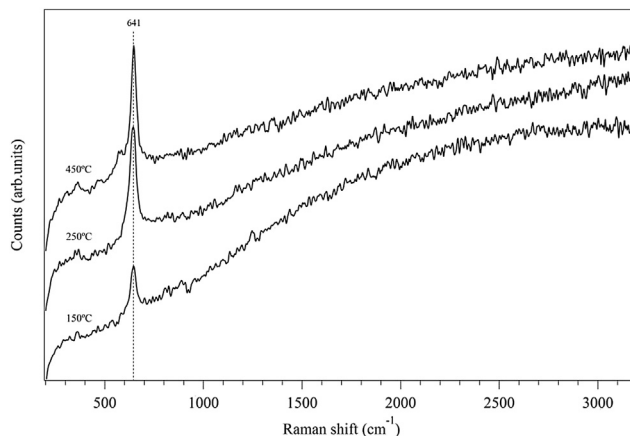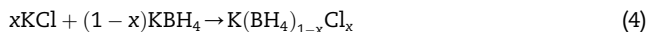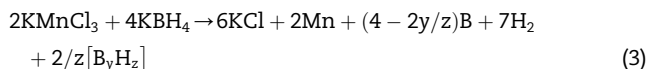The milled $2KBH_4$–$MnCl_2$ sample shows a two-step decomposition behaviour. The first between 100 and 160 °C is associated with the decomposition of $K_2Mn(BH_4)_4$ to form KBH_4, boron, finely dispersed manganese, as well as the release of hydrogen and trace diborane with a mass loss of 1.6 ± 0.1 wt%. The second between 165 and 260 °C shows several reactions taking place simultaneously: the reaction of KBH_4 (or $KCl_x(BH_4)_{1-x}$ solid solution) with ternary chloride to release hydrogen with a mass loss of 1.9 ± 0.1 wt% and to form KCl, boron, finely dispersed manganese and possibly small amounts of higher borane species; the dissolution of KCl in KBH_4 to form a $KCl_x(BH_4)_{1-x}$ solid solution phase; and the transformation of ternary chloride from $KMnCl_3$ to K_4MnCl_6.

The decomposition properties of Mn-based borohydrides highly depend on their composition and nature. The mixed-ion borohydride ($K_2Mn(BH_4)_4$) from the milled $2KBH_4$–$MnCl_2$ sample exhibits a lower decomposition temperature than that of the milled $2LiBH_4$–$MnCl_2$ sample [4], thus the combination of appropriate cations is a potential method for adjusting the thermodynamic stability of borohydrides so as to have decomposition temperatures within the desired range for hydrogen storage applications.

Acknowledgements

REFERENCES

[1] Nakamori Y, Miwa K, Ninomiya A, Li HW, Ohba N, Towata S, et al. Correlation between thermodynamical stabilities of metal borohydrides and cation electronegativites: first-principles calculations and experiments. Phys Rev B 2006;74(4):0451261–9.

[2] Nakamori Y, Li HW, Kikuchi K, Aoki M, Miwa K, Towata S, et al. Thermodynamical stabilities of metal-borohydrides. J Alloy Compd 2007;446:296–300.

[3] Černý R, Penin N, Hagernann H, Filinchuk Y. The first crystallographic and spectroscopic characterization of a 3d-metal borohydride: $Mn(BH_4)_2$. J Phys Chem C 2009;113:9003–7.

[4] Liu R, Reed D, Book D. Decomposition behaviour of $Mn(BH_4)_2$ formed by ball-milling $LiBH_4$ and $MnCl_2$. J Alloy Compd 2012;515:32–8.

[5] Liu R. Synthesis, characterization and decomposition properties of manganese – based borohydrides for hydrogen storage (PhD thesis). University of Birmingham; 2012.

[6] Hagemann H, Longhini M, Kaminski JW, Wesolowski TA, Cerny R, Penin N, et al. $LiSc(BH_4)_4$: a novel salt of Li^+ and discrete $Sc(BH_4)_4^-$ complex anions. J Phys Chem A 2008;112(33):7551–5.

[7] Li HW, Orimo S, Nakamori Y, Miwa K, Ohba N, Towata S, et al. Materials designing of metal borohydrides: viewpoints from thermodynamical stabilities. J Alloy Compd 2007;446:315–8.

[8] Nickels EA, Jones MO, David WF, Johnson SR, Lowton RL, Sommariva M, et al. Tuning the decomposition temperature in complex hydrides: synthesis of a mixed alkali metal borohydride. Angew Chem Int Ed 2008;47(15):2817–9.

[9] Ravnsbaek D, Filinchuk Y, Cerenius Y, Jakobsen HJ, Besenbacher F, Skibsted J, et al. A series of mixed-metal borohydrides. Angew Chem Int Ed 2009;48(36):6659–63.

[10] Ravnsbaek DB, Rude LH, Jensen TR. Chloride substitution in sodium borohydride. J Solid State Chem 2011;184:1858–66.

[11] Arnbjerg LM, Ravnsbæk DB, Filinchuk Y, Vang RT, Cerenius Y, Besenbacher F, et al. Structure and dynamics for $LiBH_4$–$LiCl$ solid solutions. Chem Mater 2009;21(24):5772–82.

[12] Mosegaard L, Møller B, Jørgensen JE, Filinchuk Y, Cerenius Y, Hanson JC, et al. Reactivity of $LiBH_4$: in situ synchrotron radiation powder X-ray diffraction study. J Phys Chem C 2008;112(4):1299–303.

[13] Schouwink P, D'Anna V, Ley MB, Daku LML, Richter B, Jensen TR, et al. Bimetallic borohydrides in the system $M(BH_4)_2$–KBH_4 (M = Mg, Mn): on the structural diversity. J Physical Chem C 2012;116:10829–40.

[14] Coelho AA. TOPAS, general profile and structure analysis software for powder diffraction data, version 3.0. Karlsruhe, Germany: Bruker AXS; 2004.

[15] Evans JSO. TOPAS academic [online] Available from: http://www.dur.ac.uk/john.evans/topas_academic/topas_main.htm [accessed 07.10.09].

[16] CDS Chemical crystal database [online] Available from: http://cds.dl.ac.uk [accessed 10.10.09].

[17] Gurewitz E, Melamud M, Horowitz A. Polytypism in $KMnCl_3$, neutron-diffraction study of the distorted-perovskite-structure compound. Phys Rev B 1982;25(8):5220–9.

[18] Černý R, Ravnsbaek DB, Severa G, Filinchuk Y, Hagemann H, Haase D, et al. Structure and characterization of $KSc(BH_4)_4$. J Phys Chem C 2010;114(45):19540–9.

[19] Ravnsbaek DB, Sorensen LH, Filinchuk Y, Reed D, Book D, Jakobsen HJ, et al. Mixed-anion and mixed-cation borohydride $KZn(BH_4)Cl_2$: synthesis, structure and thermal decomposition. Eur J Inorg Chem 2010;11:1608–12.

[20] Harvey KB, McQuaker NR. Infrared and Raman spectra of potassium and sodium borohydride. Can J Chem 1971;49:3272–81.

[21] Racu AM, Schoenes J, Lodziana Z, Borgschulte A, Zuttel A. High-resolution Raman spectroscopy study of phonon modes in $LiBH_4$ and $LiBD_4$. J Phys Chem A 2008;112(40):9716–22.

[22] Reed D, Book D. Recent application of Raman spectroscopy to the study of complex hydrides for hydrogen storage. Curr Opin Solid State Mater Sci 2011;15:62–72.

[23] CRCT. "FactSage FTsalt salt database: list of systems and phases" Retrieved 08 September 2009, from http://www.crct.polymtl.ca/fact/documentation/FTsalt/FTsalt_list.htm.

[24] Muetterties EL, Merrifield RE, Knoth WH, Downing JR, Miller HC. Chemistry of boranes: 3. Infrared and Raman spectra of $B_{12}H_{12}$ and related anions. J Am Chem Soc 1962;84:2506–11.

[25] Buciuman F, Patcas F, Craciun R, Zahn DRT. Vibrational spectroscopy of bulk and supported manganese oxides. Phys Chem Chem Phys 1999;1:185–90.